Journal of Forestry Research (2024) 35:11
https://doi.org/10.1007/s11676-023-01661-y

ORIGINAL PAPER

Genome wide investigation of *Hsf* gene family in *Phoebe bournei*: identification, evolution, and expression after abiotic stresses

Wenhai Liao[1,2] · Xinghao Tang[1,3] · Jingshu Li[1,2] · Qiumian Zheng[1,2] · Ting Wang[4] · Shengze Cheng[1] · Shiping Chen[1] · Shijiang Cao[1,2] · Guangqiu Cao[1,2]

Received: 18 May 2023 / Accepted: 20 June 2023 / Published online: 7 December 2023
© The Author(s) 2023

Abstract Heat shock transcription factors (Hsfs) have important roles during plant growth and development and responses to abiotic stresses. The identification and function of *Hsf* genes have been thoroughly studied in various herbaceous plant species, but not woody species, especially *Phoebe bournei*, an endangered, unique species in China. In this study, 17 members of the *Hsf* gene family were identified from *P. bournei* using bioinformatic methods. Phylogenetic analysis indicated that *PbHsf* genes were grouped into three subfamilies: A, B, and C. Conserved motifs, three-dimensional structure, and physicochemical properties of the PbHsf proteins were also analyzed. The structure of the *PbHsf* genes varied in the number of exons and introns. Prediction of *cis*-acting elements in the promoter region indicated that *PbHsf* genes are likely involved in responses to plant hormones and stresses. A collinearity analysis demonstrated that expansions of the *PbHsf* gene family mainly take place via segmental duplication. The expression levels of *PbHsf* genes varied across different plant tissues. On the basis of the expression profiles of five representative *PbHsf* genes during heat, cold, salt, and drought stress, PbHsf proteins seem to have multiple functions depending on the type of abiotic stress. This systematic, genome-wide investigation of *PbHsf* genes in *P. bournei* and their expression patterns provides valuable insights and information for further functional dissection of Hsf proteins in this endangered, unique species.

Keywords *Phoebe bournei* · *Hsf* gene family · Evolutionary analysis · Expression mechanism · Abiotic stresses

Project funding: This study was supported by the Fujian Province Seed Industry Innovation and Industrialization Project "Innovation and Industrialization Development of Precious Tree Seed Industries (*Phoebe bornei*)" (ZYCX-LY-202102), and the Sub-project of National Key R&D Program "*Phoebe bornei* Efficient Cultivation Technology" (2016YFD0600603-2).

The online version is available at http://www.springerlink.com

Corresponding editor: Tao Xu.

Supplementary Information The online version contains supplementary material available at https://doi.org/10.1007/s11676-023-01661-y.

Wenhai Liao and Xinghao Tang contributed equally to this work.

✉ Shijiang Cao
000q813040@fafu.edu.cn

✉ Guangqiu Cao
cncgq@126.com

[1] College of Forestry, Fujian Agriculture and Forestry University, Fuzhou 350002, People's Republic of China

[2] University Key Laboratory of Forest Stress Physiology, Ecology and Molecular Biology of Fujian Province, Fuzhou 350002, People's Republic of China

[3] Fujian Academy of Forestry Sciences, Fuzhou 350002, People's Republic of China

[4] College of Plant Protection, Fujian Agriculture and Forestry University, Fuzhou 350002, People's Republic of China

Introduction

Adverse environmental stresses such as cold, high temperature, drought, and salt can severely affect the seed germination, growth, development, yield, and quality of plants (Kerchev et al. 2020; Kowalczewski et al. 2020; de Medeiros et al. 2023). *Phoebe bournei* (Hemsl.) Yang, a member of the Lauraceae family, is a well-known garden tree and one of the dominant plants in broad-leaved evergreen forests of the subtropics, with a high economic value and ecological significance (Li et al. 2018; Chen et al. 2020a; Yang et al. 2020). Its timber was used for ancient palace construction and was thus a status symbol of the nobles (Ding et al. 2015, 2019; Jiao et al. 2022). In recent years, however, its growth has been hindered by human activities and abiotic stresses (Zhang et al. 2018; Li et al. 2022), resulting in a diminished population size and fragmented distribution. Currently, the species is listed as vulnerable by the IUCN and classified as a Class II key protected plant in China. Therefore, improving the tolerance of *P. bournei* so that it is better able to cope with abiotic stresses is of great importance.

Hsf is a class of transcription factors (TFs) involved in the regulation of plant defense response mechanisms under abiotic stress conditions (Guo et al. 2016). Although Hsf family members of different plant species exhibit obvious differences in protein sequence length, all share five well-conserved domains (Fig. 1A), including a conservative DNA-binding domain (DBD), an oligomerization domain (OD), also known as the HR-A/B region, a nuclear localization signal domain (NLS), activator motifs (AHAs), and a nuclear export signal domain (NES) (Guo et al. 2016; Zhang et al. 2018). The DBD is located close to the N-terminal and consists of three α-helices and four β-turns (Scharf et al. 2012), characterized by the central helix-turn-helix (H2-T-H3) motif that precisely combines the HSEs (heat shock elements) (Sakurai and Enoki 2010). The HR-A/B region comprises two hydrophobic heptad repeating regions, designated as A and B. According to the variations in the number of inserted amino acid residues present in the HR-A/B regions, plant Hsfs can be classed into three subfamilies: HsfA, HsfB, and HsfC (Nover et al. 2001). NLS and NES are located at the C-terminal of the Hsf members, which influence the subcellular localization, DNA binding, and activation functions of the Hsf. Members of HsfA possess an AHA motif, which mediates transcriptional activator function. In contrast, HsfB and HsfC members lack a motif, meaning that no self-activating function is present (Doring et al. 2000; Kotak et al. 2004). Intriguingly, the C-terminal of HsfB proteins harbors a well-conserved tetrapeptide repression domain (LFGV) (Fig. 1A) (Scharf et al. 2012).

In plants, the *Hsf* gene was first cloned in tomato (*Solanum Lycopersicum*) (Scharf et al. 1990). Since then, the *Hsf* gene family has been identified and extensively analyzed in many different species; for example, 56 *Hsf* genes have been found in wheat (*Triticum aestivum*), 52 in soybean (*Glycine max*), 30 in maize (*Zea mays*), and 21 in *Arabidopsis* (*Arabidopsis thaliana*) (Scharf et al. 2012). More importantly, the construction of several *Hsf* gene family databases has provided comprehensive

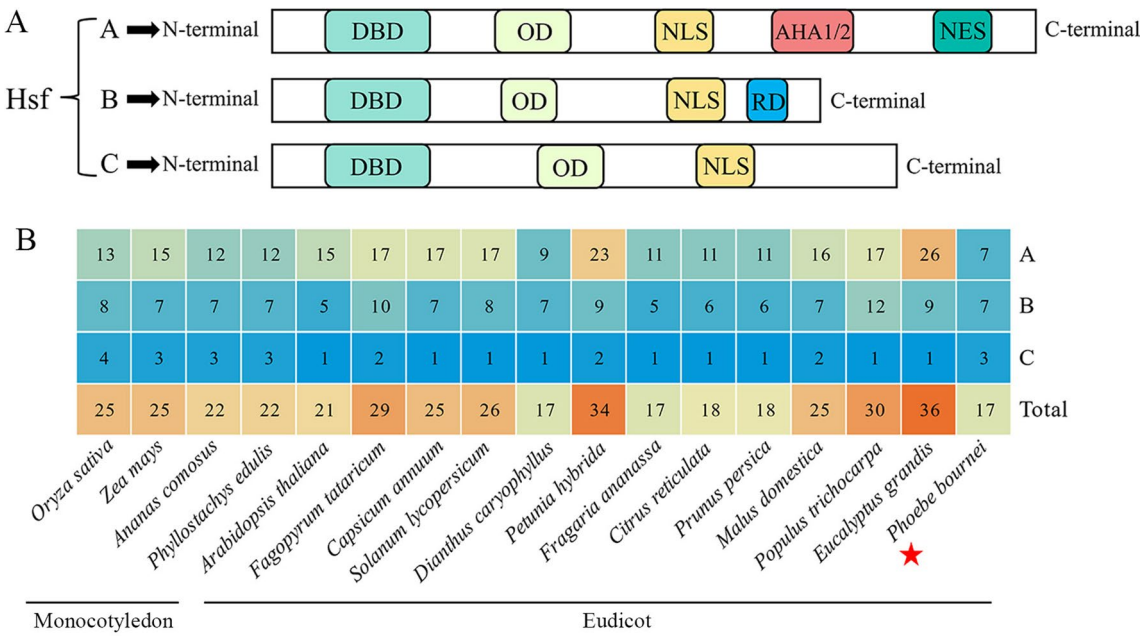


Fig. 1 Schematic diagram of the conserved structure of Hsf protein by subfamily and their distribution across plant species. **A** The three Hsf subfamilies (HsfA, HsfB, and HsfC). Rounded rectangles in different colors indicate conserved functional domains of Hsf proteins (adapted from Scharf et al. 2012). **B** The number of reported *Hsf* genes by subfamily in various plant species

information that has further aided comparative analyses of the *Hsf* gene family and provided clues to exploring their expression and evolutionary mechanisms (Ratheesh Kumar et al. 2012; Yu et al. 2022). Expression of *Hsf* genes is affected by various biotic and abiotic stress conditions, and the genes play a significant role in plant responses to stress (Dossa et al. 2016; Guo et al. 2016). As an example, *HSFA6b* in *Arabidopsis* is not only involved in a high-temperature stress response, but also acts as a positive regulator of the ABA signaling-mediated stress pathway, significantly improving the salt and drought tolerance of these plants (Huang et al. 2016). Studies have shown that most *PvHsf* genes in the common bean (*Phaseolus vulgaris*) are differentially expressed during temperature, salt, and heavy metal stress, indicating that *PvHsfs* may play specific functions depending on the specific abiotic stress (Zhang et al. 2022a). Additionally, *HsfA2* may play an important role in physiological adaptation to spaceflight (Zupanska et al. 2019). The *Hsf* gene family is also involved in regulating the growth and development processes of plants (Lin et al. 2015). In tobacco (*Nicotiana tabacum*) over-expressing *HsfA9*, the accumulation of chlorophyll increases, thus promoting photosynthesis and influencing plant growth (Prieto-Dapena et al. 2017).

In contrast to annual herbaceous plants, trees are more susceptible to sustained damage from complex natural stresses due to their prolonged life cycle, and their genetic breeding and improvement are very challenging (Borthakur et al. 2022). Among five representative *EgHsf* genes in *Eucalyptus grandis*, three are upregulated genes and two downregulated at 4 °C and two upregulated and three downregulated genes at 40 °C (Yuan et al. 2022). When the seedlings were exposed to 200 mM NaCl, all five *EgHsf* genes were upregulated after 12 h and 24 h. These results suggest that *Hsf* genes play key roles in responding to abiotic stresses in woody plants. Thus, the functions of the *Hsf* gene family in *P. bournei* need to be determined. In 2022, the sequence of the genome of *P. bournei* at the chromosome level was published, accelerating functional genomic studies (Han et al. 2022).

In the present genome-wide investigation of *Hsf* genes in *P. bournei* using bioinformatic methods, we also assessed their responses to several abiotic stresses. To the best of our knowledge, this is the first report on the *Hsf* gene family in *P. bournei*, and the findings will provide valuable genetic resources for future studies of gene function and cloning to improve the stress resistance of *P. bournei*.

Materials and methods

Identification and analysis of Hsf proteins in P. bournei

The genomic data (cDNAs and proteins) for *P. bournei* were derived from the China National GeneBank DataBase (https://db.cngb.org/), and the BioProject accession number is CNP0002030 (Han et al. 2022). The PbHsf proteins were identified using two specific methods. (1) A hidden Markov model of the conserved DBD domain of the Hsf (PF00447) was obtained from the Pfam database (http://pfam.xfam.org/) (El-Gebali et al. 2018), and the Simple HMM Search module in TBtools was used to search the Hsf protein sequences of the *P. bournei* genome (Chen et al. 2020a). (2) We used 21 AtHsf protein sequences of *Arabidopsis* that were downloaded from the Plant Transcription Factor Database (PTFD) (http://planttfdb.gao-lab.org/index.php) (Jin et al. 2017) as Hsf query sequences for a BLASTp search (E-value < 1e − 5) of all *P. bournei* protein sequences. For the respective methods, we obtained 25 and 27 candidate sequences. These PbHsf candidates were then screened a DBD domain using the online website NCBI Conserved Domain Database (NCBI-CDD) (https://www.ncbi.nlm.nih.gov/cdd/) (Marchler-Bauer et al. 2016) and SMART (http://smart.embl-heidelberg.de/) to confirm that they are Hsf sequences.

Physicochemical properties and phylogenetic tree for PbHsf proteins

Physicochemical variables of 17 PbHsf proteins were predicted using the ExPASy ProtParam online tool (https://web.expasy.org/protparam/). Subcellular localizations were predicted using the WoLF PSORT website (https://wolfpsort.hgc.jp/) (Horton et al. 2007). We obtained 21 and 25 Hsf protein sequences in *Arabidopsis* and rice (*Oryza sativa*) from the PTFD database. Then the plant Hsf protein sequences were aligned using MUSCLE with default parameters (Edgar 2004). A phylogenetic tree of all proteins was constructed via MEGA 7 software, using the neighbor-joining (NJ) method, and the bootstrap value was set to 1000. The phylogenetic tree was visualized and post-processed with iTOL (https://itol.embl.de/itol.cgi) (Letunic and Bork 2021).

Motifs and gene structure analysis of PbHsf genes

The MEME Suite 5.4.1 online tool (http://meme-suite.org/) was used to identify the conservative motifs in PbHsf proteins, while the maximum number of motifs was set to 10 with the motif sites corresponding to a ZOOPS (Zero or One Occurrence Per Sequence) model (Bailey et al. 2009). The intron–exon distributions of *PbHsf* genes were obtained using GFF annotation files from the *P. bournei* genome. The motifs and gene structure were visualized using TBtools (Chen et al. 2020a).

Sequence alignment and three-dimensional structural of PbHsf proteins

The conserved domains of PbHsf protein sequences were edited using Jalview software (Waterhouse et al. 2009). SOPMA (https://npsa-prabi.ibcp.fr/cgi-bin/npsa_automat.pl?page=npsa_sopma.html) was utilized for the protein secondary structure prediction, using default parameters. The SWISS-MODEL database (https://swissmodel.expasy.org/) was used to predict the protein tertiary structure using the homology modeling method.

Chromosomal location, gene duplication and synteny analysis of PbHsf genes

The distribution of *PbHsf* genes on the *P. bournei* genome chromosomes was mapped using the MG2C online site (http://mg2c.iask.in/mg2c_v2.1/). The genomes of five representative plants, namely *Arabidopsis*, rice, grape (*Vitis vinifera*), *Populus trichocarpa*, and *E. grandis* were downloaded from the NCBI database. Subsequently, gene duplication events, Ka/Ks ratios, and collinearity relationships with other plants were evaluated using TBtools (Chen et al. 2020a, 2022).

Cis-acting elements and the expression profiles of PbHsf genes

The upstream 2000-bp sequence of all *PbHsf* genes promoters were obtained by adding the *P. bournei* CDS file to the TBtools GFF3 Sequence Extractor submenu. Then, we uploaded the obtained 2000-bp sequence files to the PlantCARE online website (http://bioinformatics.psb.ugent.be/webtools/plantcare/html/) (Lescot et al. 2002) to predict *cis*-acting elements and visualized them using ChiPlot online tool (https://www.chiplot.online/). Transcriptome data of *PbHsf* genes in different tissues were downloaded from the NCBI, and the expression levels were shown in a cartoon-heatmap form (Chen et al. 2020c).

Plant materials and abiotic stress treatments

P. bournei seedlings, grown at 25 °C in a greenhouse with 75% relative humidity, with the same level of growth and free of pests and diseases were selected for abiotic stress treatment. Three biological replicates, each comprising two seedlings were used for each treatment: 10% PEG6000 for drought stress with a well-hydrated control group; 10% NaCl solution for salt stress with the control group in distilled water; heat stress in an incubator at 40 °C and cold stress at 10 °C, with the control group at room temperature (25 °C). *P. bournei* leaves were detached at 4, 6, 8, 12 and 24 h, immediately frozen in liquid N_2, then stored at − 80 °C until used.

RNA extraction and RT-qPCR analysis

Total RNA was extracted from the leaf samples using a HiPure Plant RNA Mini Kit (Magen, Guangdong, China). Then, cDNA was synthesized using a PrimeScript RT Reagent Kit (Perfect Real Time) (TaKaRa, Dalian, China). The obtained cDNA was then used for RT-qPCR with specific primers for the *PbHsf* genes that were designed using the Primer 3 online tool (http://bioinfo.ut.ee/primer3-0.4.0/). *PbEF1α* gene was used as a reference control (Zhang et al. 2018). Primer sequences are given in Table S1. In quick succession, the expression of *PbHsf* genes in response to abiotic stresses was quantified using RT-qPCR with a CFX Real-Time PCR System (Bio-Rad, USA) and reaction solution comprising 1 µL of cDNA, 10 µL of SYBR Premix Ex TaqTM II, 2 µL of specific primers, and 7 µL of ddH_2O. The thermocycling conditions were 95 °C for 30 s; 40 cycles at 95 °C for 5 s, 60 °C for 30 s, 95 °C for 5 s, 60 °C for 60 s, 50 °C for 30 s. Finally, the relative expression of each gene was calculated using the $2^{-\Delta\Delta CT}$ method (Livak and Schmittgen 2001) and visualized as a heatmap using TBtools (Chen et al. 2020a).

Result

Identification and physicochemical properties of PbHsf proteins

After deleting redundant sequences, we identified 17 *Hsf* genes from the *P. bournei* genome using bioinformatics methods (Fig. 2A). The *PbHsf* genes were renamed according to their phylogenetic relationship with the *Hsf* gene family in *Arabidopsis* and rice (Table 1 and Fig. 2C). The lengths of 17 PbHsf proteins varied from 214 aa (PbHsfA6a and PbHsfB3b) to 518 aa (PbHsfA8), and MW ranged from 24.49 kD (PbHsfB3b) to 58.18 kD (PbHsfA8). The theoretical pIs ranged from 4.78 (PbHsfA1a) to 10.05 (PbHsfB3b). The negative hydropathicity index of 17 PbHsf proteins suggested that they were hydrophilic. The aliphatic index ranged from 58.28 (PbHsfA4) to 83.63 (PbHsfA1b), and the instability index of PbHsf proteins ranged from 46.49 (PbHsfB3b) to 67.79 (PbHsfB3a). The subcellular localization predictions indicated that all of the PbHsf proteins were in the nucleus (Table 1).

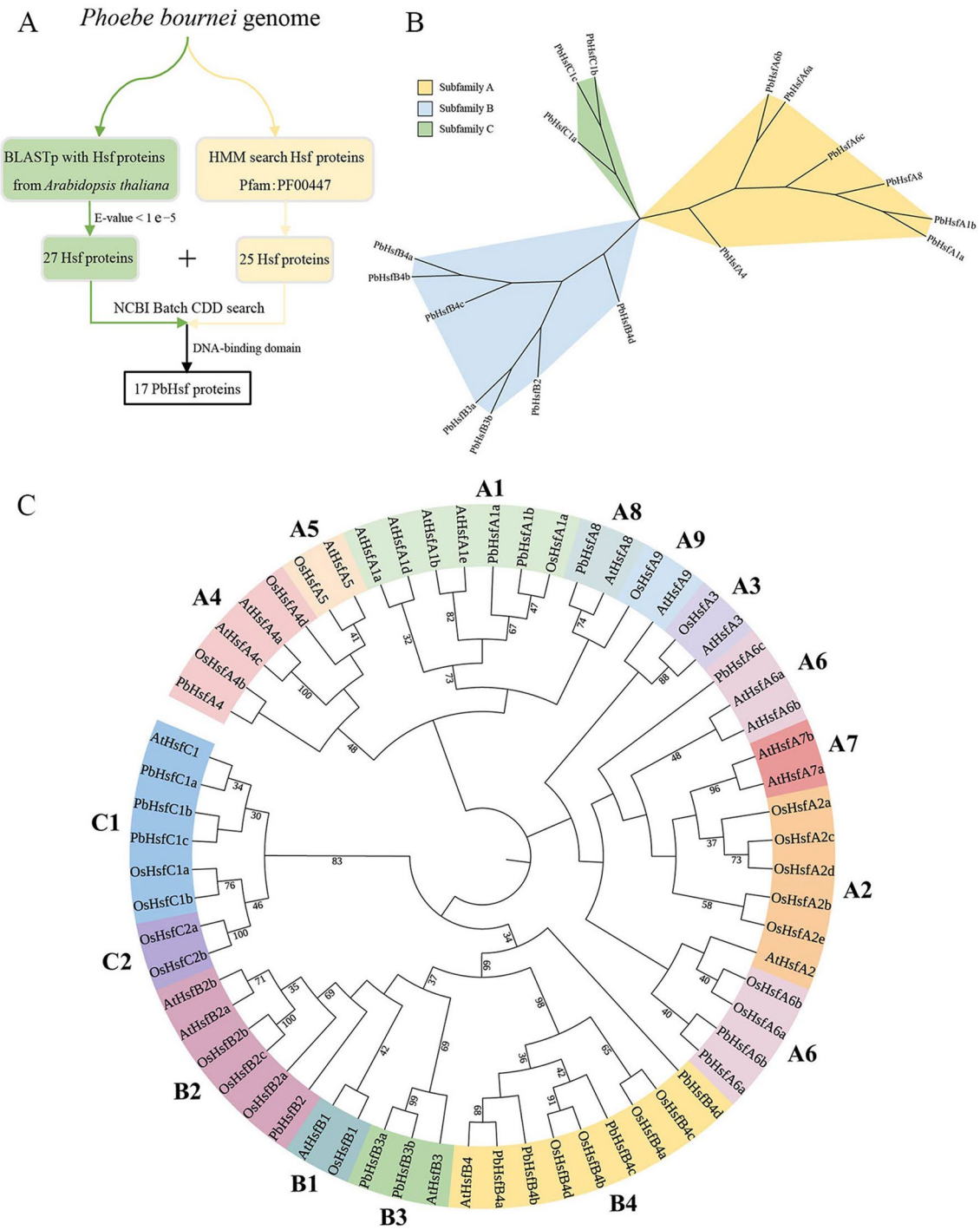


Fig. 2 Identification and evolutionary analysis of *PbHsf* genes in *Phoebe bournei*. **A** The two strategies employed in searching accurate PbHsf protein sequences. **B** Intraspecific evolutionary relationship of *PbHsf* genes. **C** Phylogenetic tree based on *Hsf* sequences from *P. bournei* (Pb), *Arabidopsis* (At), and rice (Os). Different colors represent different *Hsf* classes

Evolutionary analysis of PbHsf genes

MEGA 7 was used to analyze the protein sequences of PbHsfs through the neighbor-joining method. Based on the well-established classifications of 21 and 25 genes in *Arabidopsis* and rice Hsf families, respectively (Nover et al. 2001; Mittal et al. 2009; Scharf et al. 2012), the *Hsf* gene numbers in *P. bournei* were classified into subfamilies A, B, or C and classes A1, A4, A6, A8, B2, B3, B4, or C1 (Fig. 2C). Seven *Hsf* genes were in subfamily A and seven

Table 1 Physicochemical properties of proteins encoded by the 17 *PbHsf* genes in *Phoebe bournei*

Gene ID	Gene name	Size (aa)	MW (kDa)	pI	Instability index	Aliphatic index	GRAVY	Cellular location
OF18073-RA	*PbHsfA1a*	480	53.41	4.78	57.73	70.50	−0.613	Nucleus
OF24531-RA	*PbHsfA1b*	375	41.30	5.57	55.16	83.63	−0.376	Nucleus
OF09168-RA	*PbHsfA4*	418	47.92	5.70	58.98	58.28	−0.969	Nucleus
OF13828-RA	*PbHsfA6a*	214	24.74	6.09	56.95	68.74	−0.710	Nucleus
OF22453-RA	*PbHsfA6b*	370	41.97	4.95	53.69	72.97	−0.606	Nucleus
OF09843-RA	*PbHsfA6c*	283	33.14	8.37	64.82	66.82	−1.214	Nucleus
OF11919-RA	*PbHsfA8*	518	58.18	5.77	54.57	82.63	−0.332	Nucleus
OF18699-RA	*PbHsfB2*	265	30.28	7.65	52.88	67.70	−0.699	Nucleus
OF29691-RA	*PbHsfB3a*	232	26.40	8.79	67.79	63.49	−0.721	Nucleus
OF03667-RA	*PbHsfB3b*	214	24.49	10.05	46.49	75.14	−0.544	Nucleus
OF17747-RA	*PbHsfB4a*	345	38.38	7.77	65.92	67.86	−0.545	Nucleus
OF18687-RA	*PbHsfB4b*	334	38.04	8.63	62.19	77.01	−0.480	Nucleus
OF11677-RA	*PbHsfB4c*	280	32.28	6.31	63.47	77.25	−0.486	Nucleus
OF19445-RA	*PbHsfB4d*	303	34.85	9.07	59.67	67.56	−0.817	Nucleus
OF13659-RA	*PbHsfC1a*	225	26.66	9.27	51.67	77.11	−0.698	Nucleus
OF22691-RA	*PbHsfC1b*	314	35.40	6.88	50.23	72.58	−0.469	Nucleus
OF04246-RA	*PbHsfC1c*	243	27.57	9.58	55.77	71.07	−0.783	Nucleus

MW molecular weight, *pI* isoelectric point, *GRAVY* grand average of hydropathicity

in B, and only three were in subfamily C (Fig. 2B). In this study, among the eight *PbHsf* classes, class B4 had the most *P. bournei Hsf* genes (four), and three *Hsf* genes each in classes A6 and C1. Unlike the genes in the *AtHsf* family, none of the *PbHsf* family belonged to classes A2, A3, A5, A7, A9, or B1. In addition, class C2 was exclusive to the *OsHsf* family (Fig. 2C).

Protein motif and gene structure analysis of PbHsf genes

Ten conserved motifs in PbHsf proteins were identified and analyzed with the MEME tool (Fig. 3B). Motifs 1, 2, and 6 constituted the DBD domain and were found in most PbHsfs. Motif 1 was present in all PbHsf proteins. Although motif 3 was observed in subfamilies A and C, it was not present in subfamily B. Motifs 5, 8, and 9 were unique to subfamily B. Motif 4 was found in subfamilies A and B (except for PbHsfA4 and PbHsfB4d), rather than subfamily C. Only subfamily A contained motif 10. The exons, introns, and UTR structure of *PbHsf* genes were analyzed using TBtools (Fig. 3C). The *PbHsf* genes had from two to seven exons, with the exception of *PbHsfC1c*, which only had one. *PbHsfB4b* had a maximum of seven exons. *PbHsf* genes varied containing between one and six introns, with 10 of 17 having only one intron. Notably, one gene in subfamily C, *PbHsfC1c*, did not have any introns. The untranslated region (UTR) sequences of *PbHsf* genes in *P. bournei* were incomplete. Specifically, nine *PbHsf* genes had both 5′ UTR and 3′ UTR sequences, and one gene (*PbHsfA6b*) only had a 5′ UTR. Conversely, seven *PbHsf* genes did not have any UTR sequences.

Multiple sequence alignment and three-dimensional structure prediction of PbHsf proteins

The protein sequences of the *Hsf* gene family contain five typically conserved domains: DBD, OD, NLS, AHA, and NES from the N-terminal to the C-terminal (Fig. 1A). Among them, the DBD is the most conservative domain, containing three α-helices and four β-turns (α1-β1-β2-α2-α3-β3-β4) (Fig. 4A). To further investigate protein structures of *PbHsf* genes, we used SOPMA and SWISS-MODEL to predict their secondary and tertiary structures. Random coils and α-helices were the most frequently occurring secondary structures (Table S2). The three-dimensional structure of PbHsf proteins was generated, resulting in similar templates obtained by comparison in the Protein Data Base (Fig. 4B). The model with the highest identity, GMQE, and QMEAN score was selected as the optimal and representative protein structure from the eight classes of PbHsfs (Table S3). Each protein from the different classes had a relatively symmetrical and highly similar structure, so we can infer that the *PbHsf* genes and the functions of the three subfamilies are similar at the protein structural level.

Chromosome location, collinearity, and Ka/Ks analysis of PbHsf genes

In the present study, 17 *PbHsf* genes were distributed across 10 chromosomes in *P. bournei*, with one to six genes present

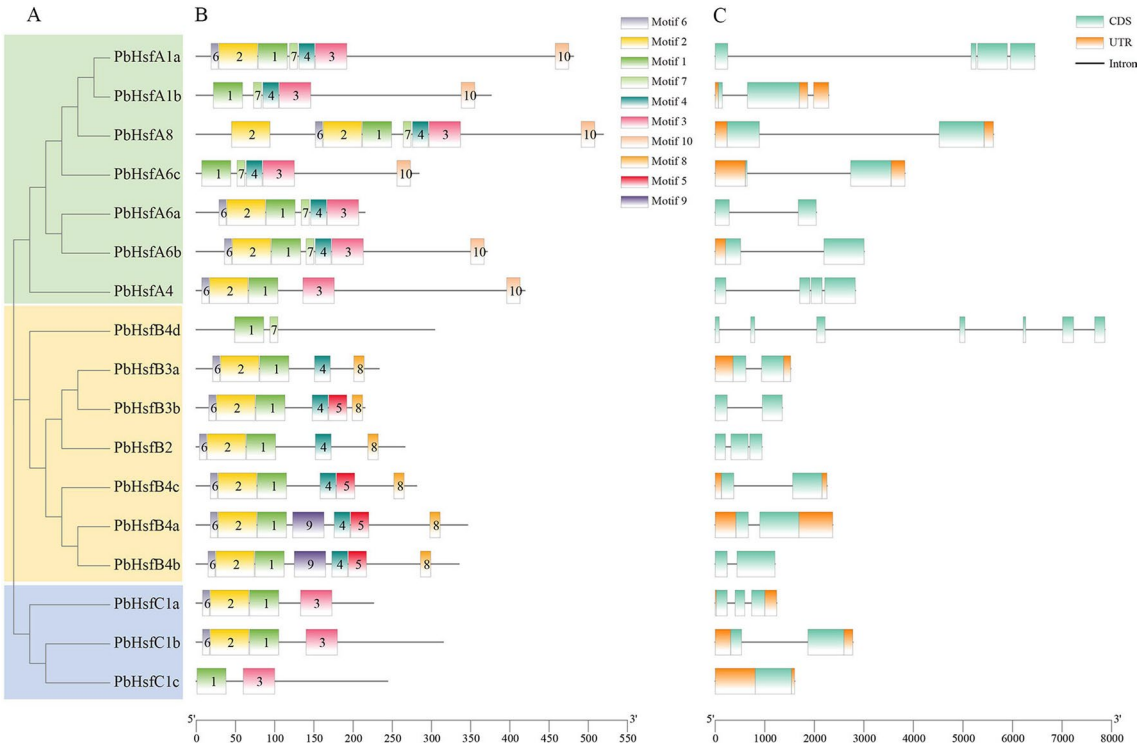


Fig. 3 Characteristics of *PbHsf* genes in *Phoebe bournei*. **A** Evolutionary relationships among *PbHsf* genes. **B** The 10 motifs of PbHsf proteins, represented as rectangles with distinct colors. **C** Gene structure of *PbHsfs*. Cyan rectangle: CDS (coding sequence), orange rectangle: UTR (untranslated region); black line: intron

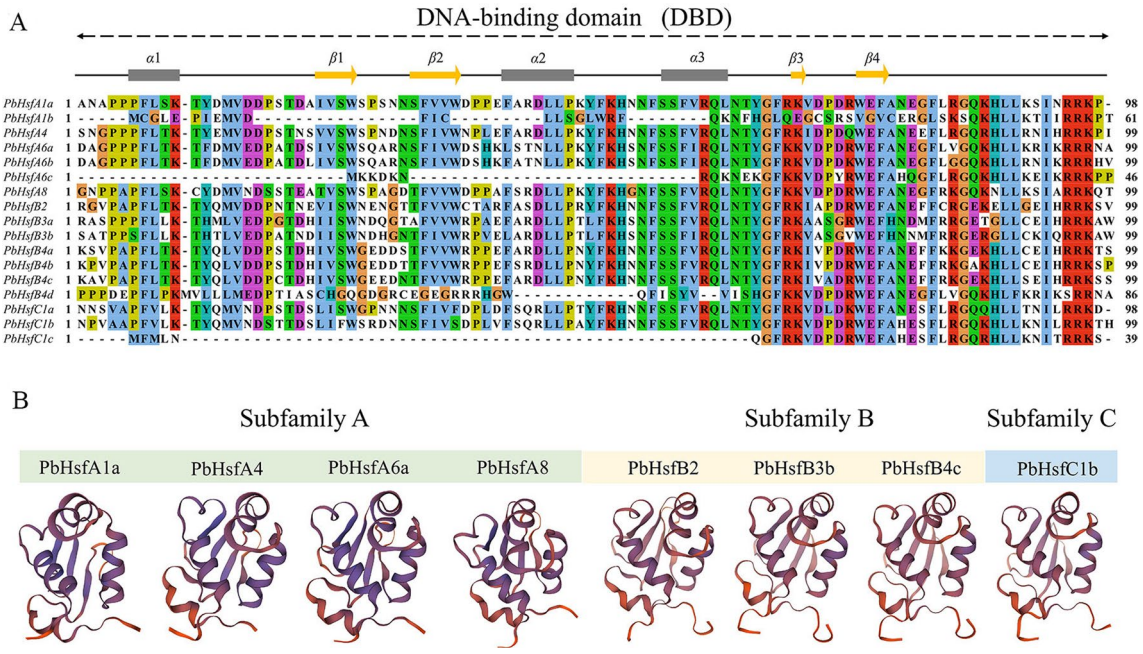


Fig. 4 Multiple sequence alignment and three-dimensional structure of PbHsf proteins in *Phoebe bournei*. **A** The DBD conserved domain of PbHsfs. **B** Three-dimensional structure of eight representative PbHsf proteins generated by the SWISS-MODEL website

on each (Fig. 5). For instance, chromosome 1 harbored the most *Hsf* genes (six), with the three subfamilies represented. In contrast, only one gene was found on chromosome 2 (subfamily C); chromosomes 3, 7, and 10 (subfamily A); and chromosomes 8, 9, and 11 (subfamily B). In addition, two genes mapped chromosomes 6 (*PbHsfB2*/*PbHsfB4b*) and 12 (*PbHsfB4d*/*PbHsfA4*), respectively. Considering the results together, the distribution of *PbHsf* genes on chromosomes is relatively uneven.

To investigate the evolution of the *Hsf* genes, the tandem and fragment duplication gene pairs of *PbHsf* gene family were studied. As shown in Fig. 5, one tandem repeat (*PbHsfB2/PbHsfB4b*) was identified on chromosome 6 as described by Holub (2001), and seven fragment repeat events were found among *PbHsf* genes, which indicates that *PbHsfs* had seven pairs of collinearity (Fig. 5B and Table S4). The fragment repeat gene pairs, *PbHsfA1a/PbHsfA1b*, *PbHsfA6a/PbHsfA6b*, and *PbHsfA1a/PbHsfA8* belonged to subfamily A, while *PbHsfB4a/PbHsfB4a* belonged to subfamily B. The three genes (*PbHsfC1a*, *PbHsfC1b*, and *PbHsfC1c*) in subfamily C are collinear with one another, forming three pairs with collinearity. Ka/Ks analysis indicated that *PbHsf* genes eliminated harmful mutations to maintain the level of purity selection (Table S4).

To analyze duplication and evolutionary processes for *PbHsf* genes, five plants were selected for comparative analysis of genome collinearity with *P. bournei*, including one monocotyledon (rice) and four dicotyledons (*Arabidopsis*, grape, *P. trichocarpa*, and *E. grandis*) (Fig. 6). A total of 22 *PbHsf* genes were collinear with those of *P. trichocarpa*, 16 with grape, 14 with *E. grandis*, nine with *A. thaliana*, and eight with rice, indicating a closer association between *P. bournei* and *P. trichocarpa*. These results clarified that the collinearity of the genome between *P. bournei* and dicotyledonous plants was greater than that between *P. bournei* and monocotyledonous plants.

Analysis of cis-acting elements in promoter of PbHsf genes

In the promoter region of the *PbHsf* genes, 32 *cis*-acting elements were identified (Fig. 7; Table S5). These *cis*-acting elements were found to be associated with hormones (nine), light (nine), plant growth and development (five), and stress (nine). The MYC element was detected in 17 *PbHsf* genes, and was the most frequently found *cis*-acting element (Fig. 7). Other *cis*-acting elements, found in 15 *PbHsf* genes, included ABRE, G-box, ARE, and WRE3. The most frequent type of element was the hormone-response type (191), including abscisic acid (ABRE), MeJA (CGTCA-motif and TGACG-motif), gibberellin (GARE-motif, MYC, P-box, and TATC-box), salicylic acid (TCA-element), auxin (TGA-element) (Table S5). The stress-response type, such as defense and stress (STRE and TC-rich repeats), low temperature (LTR), and anaerobic induction (ARE), was the second most frequent (175). A considerable number of *cis*-acting elements were light-response (152) or growth-and-development types (71) (Table S5).

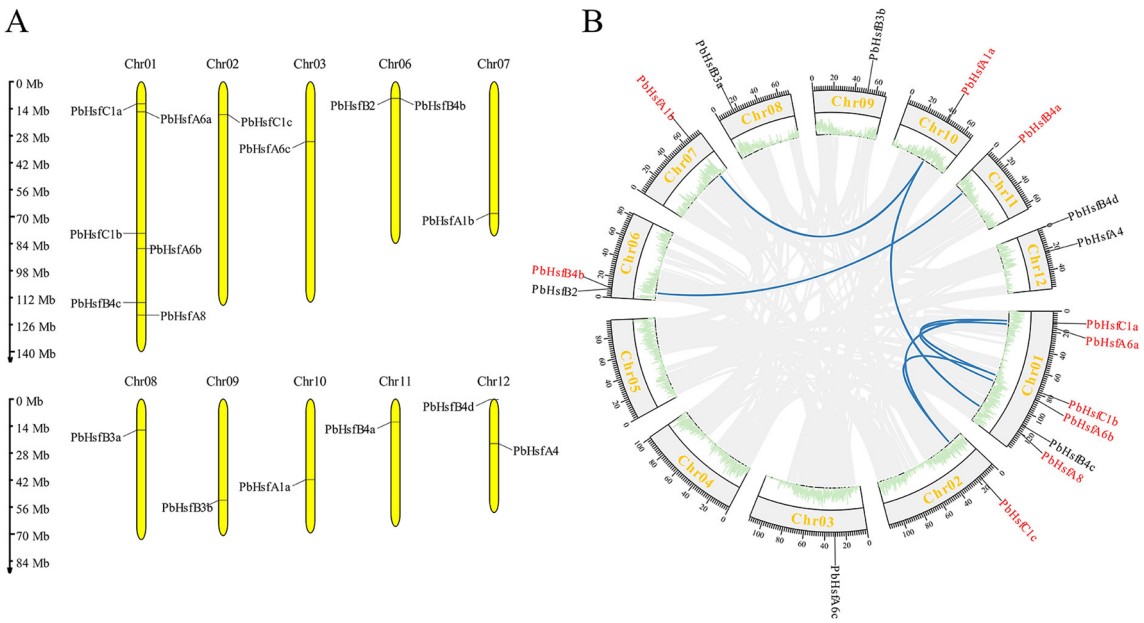


Fig. 5 Chromosome locations and collinearity of *PbHsf* genes in *Phoebe bournei*. chr: chromosome. **A** Distribution of *PbHsf* genes. *P. bournei* has 12 chromosomes; no *PbHsf* genes were mapped to chromosomes 4 and 5. **B** The green lines of the internal ring represent the density of genes per chromosome. Collinear genes are depicted by light grey lines; *PbHsf* gene pairs are shown as blue lines

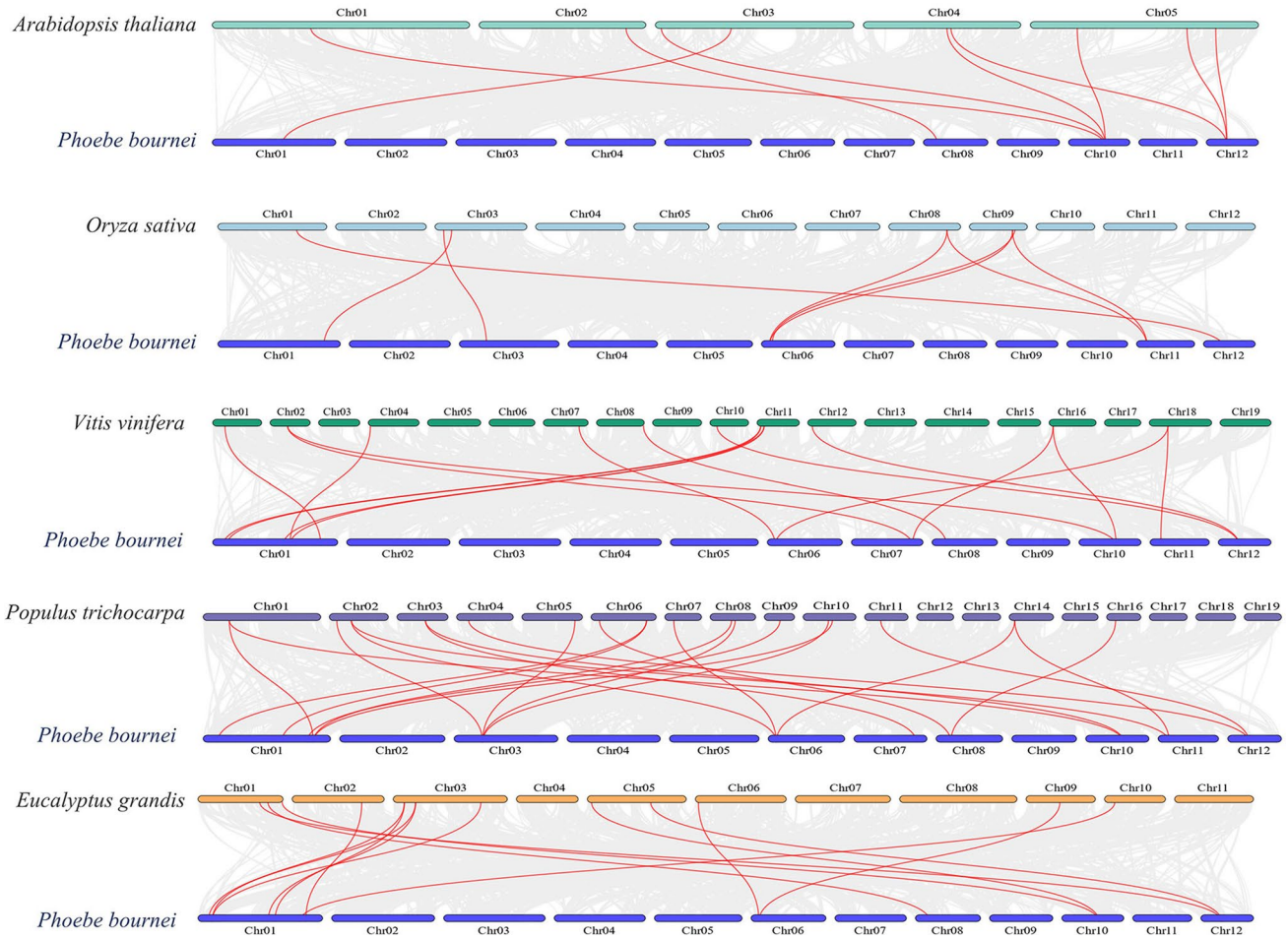


Fig. 6 *Hsf* gene collinearity analysis of *Phoebe bournei* with five plants. Red lines in the background highlight collinear *Hsf* gene pairs in *P. bournei* and plant genomes

Different tissue-specific expression analysis of PbHsf genes

To explore the functional divergence of *Hsf* genes, tissue-specific expression levels of *PbHsf* genes in root bark, root xylem, stem bark, stem xylem, and leaf were obtained from the NCBI database (Fig. 8; Table S6). In general, the expression profiles of *PbHsf* genes in the bark and xylem tissues of the stem were similar to those of the root, except for *PbHsfA6c*, which was highly expressed in stem bark. Additionally, six of 17 *PbHsf* genes, including *PbHsfA1a*, *PbHsfA6c*, and *PbHsfC1c*, were highly expressed in leaves. On the contrary, the expression of *PbHsf* genes of subfamily B was low in leaves. Five of the *PbHsf* genes were barely expressed in any of the tissues, especially *PbHsf3B*, with a notable lack of expression within the five tissues. Thus, the expression levels of the different genes differed significantly among the different tissues.

The expression profiles of PbHsf genes under abiotic stresses

To investigate the responses of *PbHsf* genes to drought, salt, or temperature stress, five representative genes (*PbHsfA1a*, *PbHsfA6c*, *PbHsfB3a*, *PbHsfB4d*, and *PbHsfC1b*) from three subfamilies were selected for RT-qPCR observation (Fig. 9; Table S7). Among them, *PbHsfA1a*, *PbHsfA6c*, and *PbHsfC1b* were highly expressed in leaves, whereas expression of *PbHsfB3a* and *PbHsfB4d* was very low (Fig. 8). Moreover, all five representative genes had a high number of stress-related *cis*-acting elements (Fig. 7). Under drought treatment (10% PEG6000), *PbHsfA1a* and *PbHsfA6c* were upregulated after 4, 6, and 8 h, while *PbHsfB3a* was upregulated after 12 and 24 h of stress. Compared with the control group (0 h), *PbHsfB4d* was downregulated within all sampling periods, and expression declined as the treatment duration increased (Fig. 9).

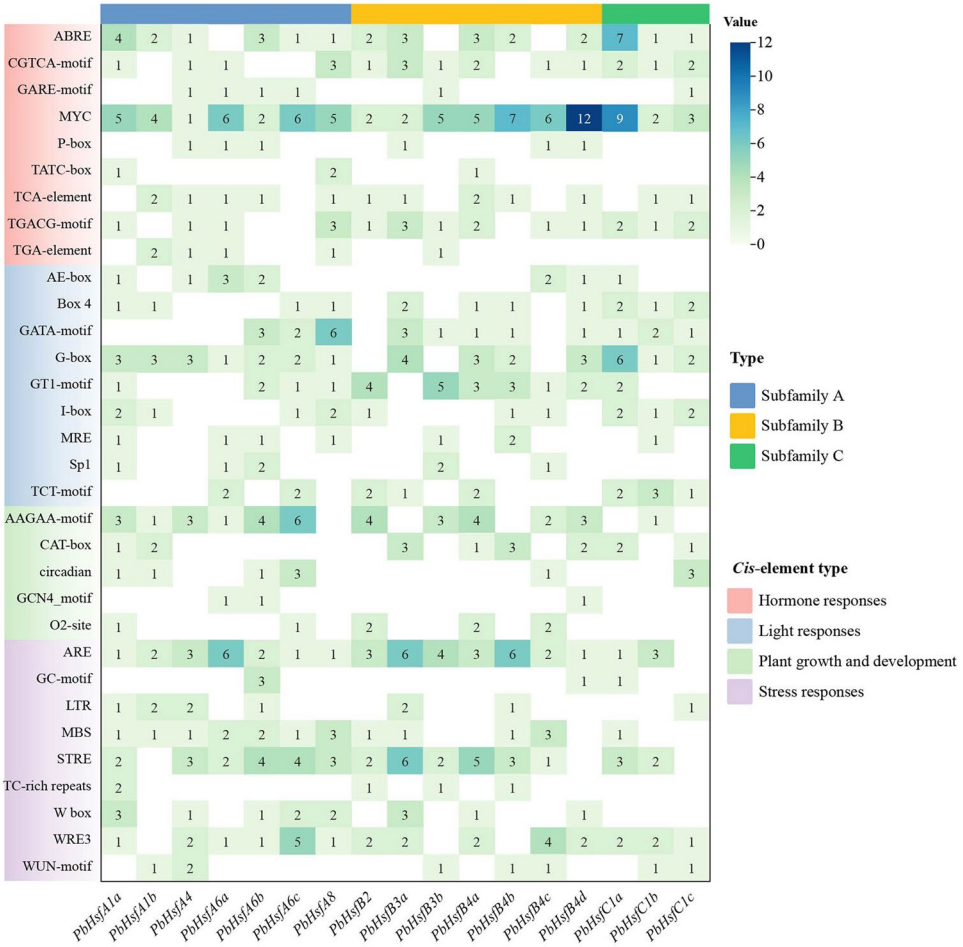


Fig. 7 Number of *cis*-acting elements in the promoter region of *PbHsf* genes in *Phoebe bournei*. Hormone responses, light responses, plant growth-development, and stress responses are shaded in different colors

In the salt treatment (10% NaCl solution), expression of *PbHsfA1a*, *PbHsfA6c*, and *PbHsfC1b* was low and were downregulated throughout all sampling periods. In contrast, the expression of *PbHsfB3a* increased significantly after 4 h and continued to increase, suggesting a potential role for *PbHsfB3a* as a key gene involved in the response to salt stress. In addition, the expression of *PbHsfB4d* was upregulated only at 4 h and downregulated at other periods (Fig. 9). During cold stress (10 °C), the expression of all five genes was upregulated and peaked at 12 h and. However, there were slight differences in expression among *PbHsf* genes during the other sampling periods. Interestingly, the expression of all five *PbHsf* genes were significantly downregulated during the heat stress (40 °C), especially *PbHsfB3a* and *PbHsfB4d*, which was severely downregulated (Fig. 9).

Discussion

The widely distributed and specific Hsf transcription factors in plants have a conserved DBD domain, which has important roles in plant growth, development, and stress responses (von Koskull-Döring et al. 2007; Andrási et al. 2020). Extensive studies of the *Hsf* gene family in many plants, especially woody plants, have benefited from the increasing availability of genome sequences. For example, 21 *Hsf* genes have been reported for *Arabidopsis* (21) (Nover et al. 2001; Scharf et al. 2012), 25 for rice (Mittal et al. 2009), 25 for apple (*Malus pumila*) (Giorno et al. 2012), 30 for poplar (*Populus*) (Zhao et al. 2023), 22 for pineapple (*Ananas comosus*) (Wang et al. 2021), and 36 for *E. grandis* (Yuan et al. 2022) (Fig. 1B). However, a comprehensive investigation of the *Hsf* gene family in *P. bournei* has not yet been published.

In the present study, we identified 17 *Hsf* genes from the *P. bournei* genome (Fig. 2), which were unevenly distributed on 10 of 12 *P. bournei* chromosomes, with the highest gene number comprising six *PbHsfs*, detected on chromosome 1 (Fig. 5). In angiosperms, three subfamilies (A, B, C) of the *Hsf* gene family consist of seven, five, and two classes, respectively (A1–A9, B1–B5, and C1–C2) (Wang et al. 2018). As previously mentioned, the *HsfC2* class exists only in monocotyledons and is absent in dicotyledons (Wang et al. 2018). The *HsfC2* class was not found in *P. bournei* and *Arabidopsis*, and two members of *OsHsf* belonged to the

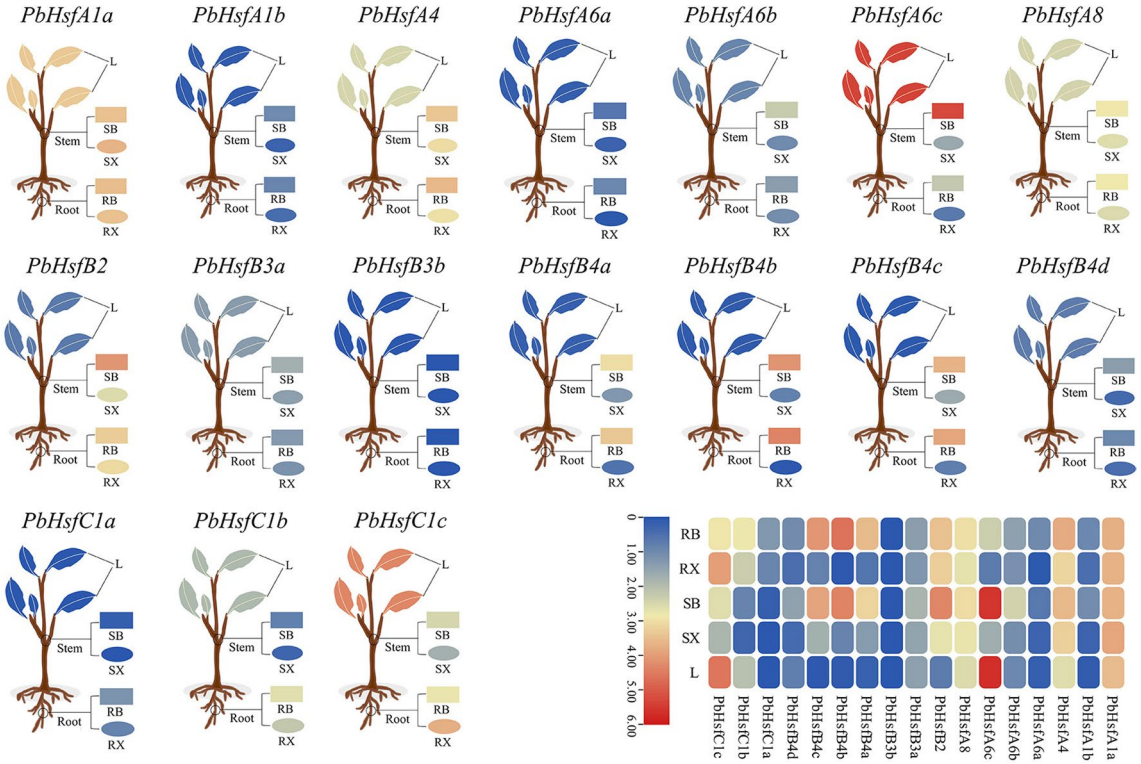


Fig. 8 Differential expression of *PbHsf* genes in different tissues of *Phoebe bournei*. RB, root bark; RX, root xylem; SB, stem bark; SX, stem xylem; L, leaves. Expression data are presented as $\log_2$ (FPKM + 1) values. Red indicates high expression of *PbHsf* genes; blue indicates low expression

HsfC2 class in rice (Fig. 2C). Therefore, the *Hsf* gene family in monocotyledons generally have more subfamily C members than in dicotyledons (Fig. 1B). Interestingly, class B5 is absent from all three of the aforementioned plants, suggesting that it is relatively rare. The physicochemical properties of PbHsf proteins vary greatly, but they are all located in the nucleus (Table 1) as found for poplar (Zhao et al. 2023) and *E. grandis* (Yuan et al. 2022).

PbHsf protein members that are closely related in the phylogenetic tree had common motif arrangements and compositions (Fig. 3). Motifs 1, 2, and 6, constituting the DBD domain, were present in almost all PbHsfs. The DBD domain was the most conserved, with three α-helices and four β-turns (α1-β1-β2-α2-α3-β3-β4) (Scharf et al. 2012; Guo et al. 2016) (Fig. 4A). Similarly, *Hsf* genes in three subfamilies had similar motifs in *Populus* (Zhang et al. 2015) and peach (*Prunus persica*) (Tan et al. 2021). In plants, introns mediate gene expression regulation (Le Hir et al. 2003; Shaul 2017). Therefore, it is of great significance to elucidate gene function by analyzing the intron structure. The gene structure analysis of *PbHsf* members revealed that all *PbHsf* genes but one contained at least one or more introns; *PbHsfC1c* had none (Fig. 3C). However, the intron length of *Hsf* genes varied to certain degrees in each subfamily, and the structure of each member differed significantly, which further affected their expression in plant tissues (Fig. 8).

Gene duplication events and collinearity relationships can help reveal gene expansion and evolution of the *PbHsf* gene family (Cannon et al. 2004). Notably, only one tandem duplication event was found in *PbHsf* genes, but segmental duplication had occurred in seven gene pairs, involving 10 *PbHsf* genes and six chromosomes. These results suggest that fragment replication events may a driving force for the expansion of the *Hsf* gene family in *P. bournei*. Subsequently, we calculated the Ka/Ks ratios of seven *PbHsf* gene pairs and found that they were all less than one (Table S4), indicating purified selection pressure during the evolutionary process. Comparable results have been reported for poplar (Zhao et al. 2023) and maize (Lin et al. 2011).

Cis-acting elements are critical in multiple biological signal transduction and stress responses (Ibraheem et al. 2010). In this study, many *cis*-acting elements were identified in the promoter regions of *PbHsf* genes and were associated with hormone regulation and stress response (Fig. 7). Gibberellin (MYC, P-box, etc.), which is important throughout the life of flowering plants, promotes seed germination and the division and the elongation of root cells (Sun 2011). Abscisic acid (ABRE) participates in plant stress response and other physiological processes such as bud dormancy and osmotic

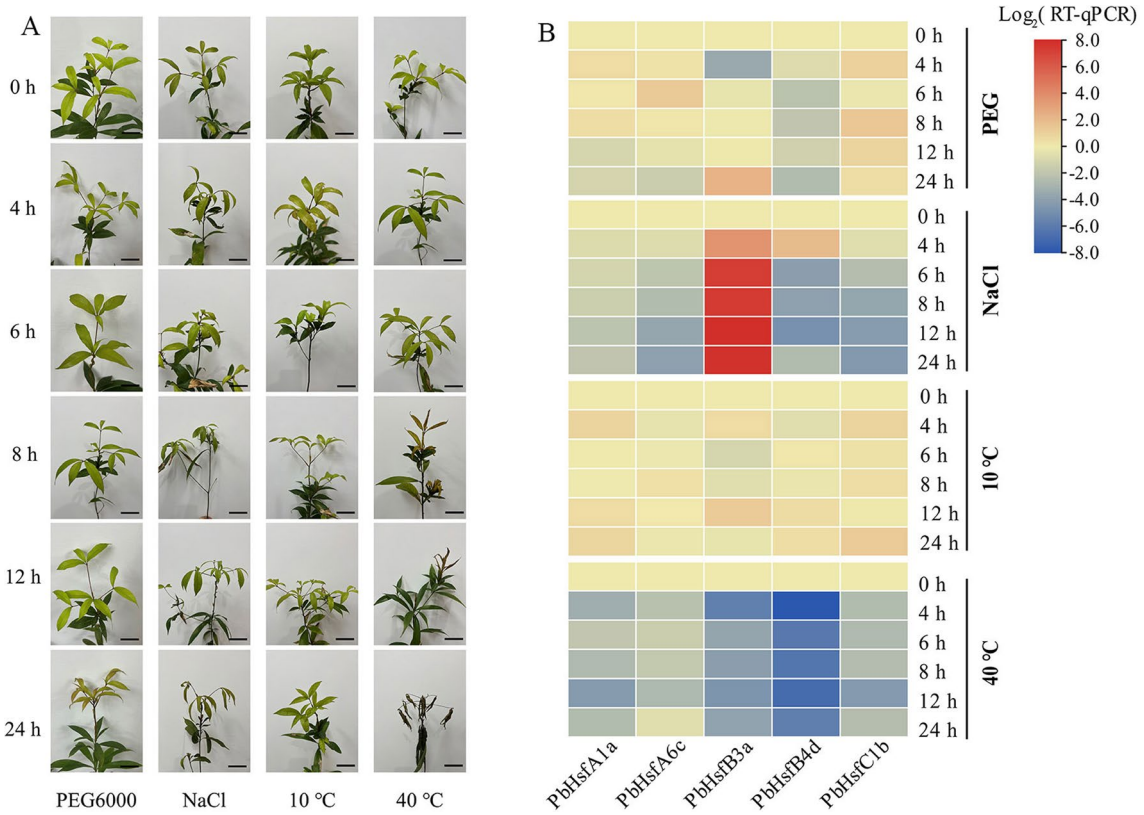


Fig. 9 Expression of five representative *PbHsf* genes in seedlings of *Phoebe bournei* response to drought, salt or temperature stress. **A** Phenotypic changes in seedlings after 0, 4, 6, 8, 12, and 24 h of treatment. Samples collected at 0 h were used as the controls. Scale bars = 40 mm. **B** Relative expression of *PbHsf* genes determined by RT-qPCR. Blue: downregulated genes; red: upregulated genes

regulation (Chen et al. 2020b). There may be a link between hormone regulation and response to abiotic stress: for example, in *PbHsfB3a*, the promoter region had six AREs, six STREs, three ABREs, and two MYCs (Fig. 7), and more importantly, the gene was upregulated during drought, salt, and cold stress (Fig. 9). However, the relationship of the gene to stress responses is uncertain, and further research is required. In addition, the presence of the G-box, GATA motif, and GT1 motif indicates that the *PbHsf* genes might be involved in light responses (Fig. 7).

The various combinations of stresses, particularly abiotic stresses, that affect plants alter the expression of different *Hsf* gene members (Nishizawa et al. 2006; Sakurai and Enoki 2010). For instance, drought, salinity, and heat stresses alter the expression of *CarHsf* genes in chickpea (*Cicer arietinum*) (Chidambaranathan et al. 2018), and stresses such as powdery mildew, drought, salt, and hormone treatments distinctly change the expression of 17 *FvHsf* genes in strawberry (Hu et al. 2015). In our RT-qPCR assays to investigate the expression profiles of five representative *PbHsf* genes after drought, salt, cold, or heat treatments, we found that *PbHsfA1a* and *PbHsfA6c* respond early to drought treatment, while *PbHsfB3a* did not increase until 24 h. In addition, *PbHsfC1b* responded positively to drought treatment (Fig. 9).

Enhancing the salt tolerance of woody plants is a research hotspot as soil salinization continues to increase around the world (Polle and Chen 2015; Guo et al. 2021, 2023). As part of this goal, Guo et al. (2023) used transcriptome data of poplar under salt stress to find that a key *Hsf* gene, *PtHsf21*, is upregulated in leaves and stems (Guo et al. 2023). Among five representative *PbHsf* genes in *P. bournei*, the performance of *PbHsfB3a* expression was about 13-fold higher than the control group after 4 h of slat stress and continued to be upregulated (Table S7 and Fig. 9). Presumably, *PbHsfB3a* carries out significant function during salt stress.

Plant growth and development are also very sensitive to temperature; even small changes can cause remarkable responses in plants (Penfield 2008). Among five randomly selected *PeHSF* genes from passion fruit (*Passiflora edulis*), the expression of all *PeHSF* genes under heat (45 °C) and osmotic (mannitol) stress increased at 12 h of treatment (Wang et al. 2023). In the present study, *PbHsf* genes in *P. bournei* had diverse expression responses to cold and heat stresses (Fig. 9), similar to changes in the expression profiles in other plants, illustrating that they are characterized

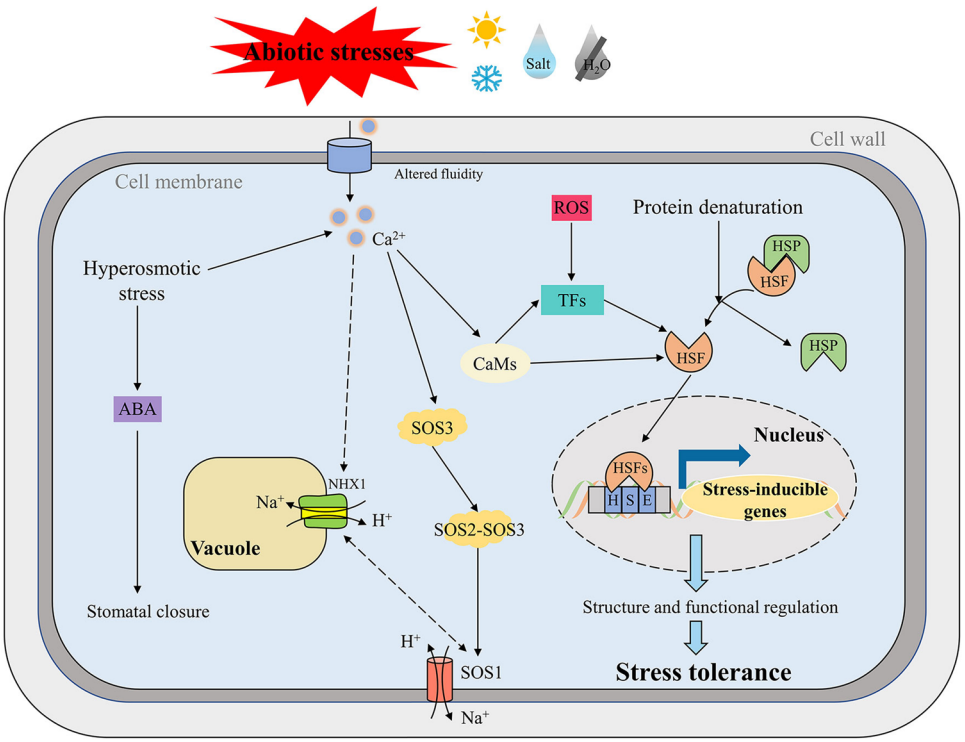


Fig. 10 Working model for the role of Hsf transcription factor during abiotic stresses and schematic diagram of plant cell response to stresses (modified from Guo et al. 2016; Zhang et al. 2022b; Ali et al. 2023). The abiotic stress induces Ca^{2+} concentration increase, ROS accumulation, and protein degradation, and subsequently signal transmission to the nucleus. The Hsf then specifically binds to the heat shock element (HSE) in the promoter region of the *Hsf* gene and activates the expression of stress-inducible genes, thereby enhancing stress tolerance in plants. ABA, abscisic acid; SOS, salt overly sensitive; CaM, Ca^{2+}-calmodulin; ROS, reactive oxygen species; TFs, transcription factors; HSF, heat shock transcription factor; HSP, heat shock protein; HSE, heat shock element

by similar cell signaling and cellular processes. Accumulating evidence thus suggests that the *Hsf* gene family, as a core part of the signal transduction, plays a key role in plant coordination and adaptation to numerous abiotic stresses (Fig. 10) (Scharf et al. 2012; Guo et al. 2016).

Conclusions

In our genome wide investigation of the *Hsf* gene family of *P. bournei*, we identified 17 *PbHsf* genes, which were classified among three subfamilies and had considerable evolutionary divergence. Tissue-specific expression profiles of the genes indicated potentially divergent functions in the growth and development of *P. bournei*. The analysis of *cis*-acting elements and gene expression patterns during various stresses suggest that the *PbHsf* genes are involved in responses to diverse abiotic stresses. Our research provides a basis for the further functional characterization of *PbHsf* genes and eventually increasing the yield and quality of *P. bournei* and other woody plants.

Open Access This article is licensed under a Creative Commons Attribution 4.0 International License, which permits use, sharing, adaptation, distribution and reproduction in any medium or format, as long as you give appropriate credit to the original author(s) and the source, provide a link to the Creative Commons licence, and indicate if changes were made. The images or other third party material in this article are included in the article's Creative Commons licence, unless indicated otherwise in a credit line to the material. If material is not included in the article's Creative Commons licence and your intended use is not permitted by statutory regulation or exceeds the permitted use, you will need to obtain permission directly from the copyright holder. To view a copy of this licence, visit http://creativecommons.org/licenses/by/4.0/.

References

Ali A, Petrov V, Yun DJ, Gechev T (2023) Revisiting plant salt tolerance: novel components of the SOS pathway. Trends Plant Sci 28(9):1060–1069. https://doi.org/10.1016/j.tplants.2023.04.003

Andrási N, Pettkó-Szandtner A, Szabados L (2020) Diversity of plant heat shock factors: regulation, interactions, and functions. J Exp Bot 72(5):1558–1575

Bailey TL, Boden M, Buske FA, Frith M, Grant CE, Clementi L, Ren J, Li WW, Noble WS (2009) MEME Suite: tools for motif discovery and searching. Nucleic Acids Res 37(suppl_2):W202–W208

Borthakur D, Busov V, Cao XH, Du QZ, Gailing O, Isik F, Ko JH, Li CH, Li QZ, Niu SH, Qu GZ, Vu THG, Wang XR, Wei ZG, Zhang L, Wei HR (2022) Current status and trends in forest genomics. For Res 2:11. https://doi.org/10.48130/FR-2022-0011

Cannon SB, Mitra A, Baumgarten A, Young ND, May G (2004) The roles of segmental and tandem gene duplication in the evolution of large gene families in *Arabidopsis thaliana*. BMC Plant Biol 4(1):10

Chen CJ, Chen H, Zhang Y, Thomas HR, Frank MH, He Y, Xia R (2020a) TBtools: an integrative toolkit developed for interactive analyses of big biological data. Mol Plant 13(8):1194–1202

Chen K, Li GJ, Bressan RA, Song CP, Zhu JK, Zhao Y (2020b) Abscisic acid dynamics, signaling, and functions in plants. J Integr Plant Biol 62(1):25–54

Chen SP, Sun WH, Xiong YF, Jiang YT, Liu XD, Liao XY, Zhang DY, Jiang SZ, Li Y, Liu B, Ma L, Yu X, He L, Liu B, Feng JL, Feng

LZ, Wang ZW, Zou SQ, Lan SR, Liu ZJ (2020c) The *Phoebe* genome sheds light on the evolution of magnoliids. Hortic Res 7(1):146

Chen CJ, Wu Y, Xia R (2022) A painless way to customize Circos plot: From data preparation to visualization using TBtools. iMeta 1(3):35

Chidambaranathan P, Jagannadham PTK, Satheesh V, Kohli D, Basavarajappa SH, Chellapilla B, Kumar J, Jain PK, Srinivasan R (2018) Genome-wide analysis identifies chickpea (*Cicer arietinum*) heat stress transcription factors (Hsfs) responsive to heat stress at the pod development stage. J Plant Res 131(3):525–542

de Medeiros RLS, de Paula RC, de Souza JVO, Pedro J (2023) Abiotic stress on seed germination and plant growth of *Zeyheria tuberculosa*. J For Res. https://doi.org/10.1007/s11676-023-01608-3

Ding YJ, Zhang JH, Lu YF, Ep L, Lou LH, Tong ZK (2015) Development of EST-SSR markers and analysis of genetic diversity in natural populations of endemic and endangered plant *Phoebe chekiangensis*. Biochem Syst Ecol 63:183–189

Ding X, Xiao JH, Li L, Conran JG, Li J (2019) Congruent species delimitation of two controversial gold-thread nanmu tree species based on morphological and restriction site-associated DNA sequencing data. J Syst Evol 57(3):234–246

Doring P, Treuter E, Kistner C, Lyck R, Chen A, Nover L (2000) The role of AHA motifs in the activator function of tomato heat stress transcription factors HsfA1 and HsfA2. Plant Cell 12(2):265–278

Dossa K, Diouf D, Cissé N (2016) Genome-wide investigation of Hsf genes in Sesame reveals their segmental duplication expansion and their active role in drought stress response. Front Plant Sci 7:1522

Edgar RC (2004) MUSCLE: multiple sequence alignment with high accuracy and high throughput. Nucleic Acids Res 32(5):1792–1797

El-Gebali S, Mistry J, Bateman A, Eddy SR, Luciani A, Potter SC, Qureshi M, Richardson LJ, Salazar GA, Smart A, Sonnhammer ELL, Hirsh L, Paladin L, Piovesan D, Tosatto SCE, Finn RD (2018) The Pfam protein families database in 2019. Nucleic Acids Res 47(D1):D427–D432. https://doi.org/10.1093/nar/gky995

Giorno F, Guerriero G, Baric S, Mariani C (2012) Heat shock transcriptional factors in *Malus domestica*: identification, classification and expression analysis. BMC Genomics 13(1):639

Guo M, Liu JH, Ma X, Luo DX, Gong ZH, Lu MH (2016) The plant heat stress transcription factors (HSFs): Structure, regulation, and function in response to abiotic stresses. Front Plant Sci 7:114

Guo Q, Jiang JH, Yao WJ, Li L, Zhao K, Cheng ZH, Han LB, Wei R, Zhou BR, Jiang TB (2021) Genome-wide analysis of poplar HD-zip family and over-expression of PsnHDZ63 confers salt tolerance in transgenic Populus simonii × P. nigra. Plant Sci 311:111021. https://doi.org/10.1016/j.plantsci.2021.111021

Guo Q, Wei R, Xu M, Yao WJ, Jiang JH, Ma XJ, Qu GZ, Jiang TB (2023) Genome-wide analysis of HSF family and overexpression of PsnHSF21 confers salt tolerance in Populus simonii×P. nigra. Front Plant Sci 14:1160102

Han X, Zhang JH, Han S, Chong SL, Meng GL, Song MY, Wang Y, Zhou SC, Liu CC, Lou LH, Lou XZ, Cheng LJ, Lin E, Huang HH, Yang Q, Tong ZK (2022) The chromosome-scale genome of *Phoebe bournei* reveals contrasting fates of terpene synthase (TPS)-a and TPS-b subfamilies. Plant Commun 3(6):100410

Holub EB (2001) The arms race is ancient history in *Arabidopsis*, the wildflower. Nat Rev Genet 2:516–527

Horton P, Park KJ, Obayashi T, Fujita N, Harada H, Adams-Collier CJ, Nakai K (2007) WoLF PSORT: protein localization predictor. Nucleic Acids Res 35(suppl_2):W585–W587

Hu Y, Han YT, Wei W, Li YJ, Zhang K, Gao YR, Zhao FL, Feng JY (2015) Identification, isolation, and expression analysis of heat shock transcription factors in the diploid woodland strawberry *Fragaria vesca*. Front Plant Sci 6:736

Huang YC, Niu CY, Yang CR, Jinn TL (2016) The heat stress factor HSFA6b connects ABA signaling and ABA-mediated heat responses. Plant Physiol 172(2):1182–1199

Ibraheem O, Botha CEJ, Bradley G (2010) In silico analysis of cis-acting regulatory elements in 5' regulatory regions of sucrose transporter gene families in rice (*Oryza sativa* Japonica) and *Arabidopsis thaliana*. Comput Biol Chem 34(5):268–283

Jiao LC, Lu Y, Zhang M, Chen YP, Wang ZS, Guo Y, Xu C, Guo J, He T, Ma LY, Gao WQ, Wang J, Zhou SL, Zhang YG, Jiang XM, Baas P, Yin YF (2022) Ancient plastid genomes solve the tree species mystery of the imperial wood "Nanmu" in the Forbidden City, the largest existing wooden palace complex in the world. Plants People Planet 4(6):696–709

Jin JP, Tian F, Yang DC, Meng YQ, Kong L, Luo JC, Gao G (2017) PlantTFDB 4.0: toward a central hub for transcription factors and regulatory interactions in plants. Nucleic Acids Res 45(D1):D1040–D1045

Kerchev P, van der Meer T, Sujeeth N, Verlee A, Stevens CV, Van Breusegem F, Gechev T (2020) Molecular priming as an approach to induce tolerance against abiotic and oxidative stresses in crop plants. Biotechnol Adv 40:107503

Kotak S, Port M, Ganguli A, Bicker F, Von Koskull-Döring P (2004) Characterization of C-terminal domains of *Arabidopsis* heat stress transcription factors (Hsfs) and identification of a new signature combination of plant class A Hsfs with AHA and NES motifs essential for activator function and intracellular localization. Plant J 39(1):98–112

Kowalczewski PŁ, Radzikowska D, Ivanišová E, Szwengiel A, Kačániová M, Sawinska Z (2020) Influence of abiotic stress factors on the antioxidant properties and polyphenols profile composition of green barley (Hordeum vulgare L.). Int J Mol Sci 21(2):397

Le Hir H, Nott A, Moore MJ (2003) How introns influence and enhance eukaryotic gene expression. Trends Biochem Sci 28(4):215–220

Lescot M, Déhais P, Thijs G, Marchal K, Moreau Y, Van de Peer Y, Rouzé P, Rombauts S (2002) PlantCARE, a database of plant cis-acting regulatory elements and a portal to tools for in silico analysis of promoter sequences. Nucleic Acids Res 30(1):325–327

Letunic I, Bork P (2021) Interactive Tree Of Life (iTOL) v5: an online tool for phylogenetic tree display and annotation. Nucleic Acids Res 49(W1):W293–W296

Li YG, Liu XH, Ma JW, Zhang XM, Xu LA (2018) Phenotypic variation in *Phoebe bournei* populations preserved in the primary distribution area. J Forestry Res 29:35–44

Li X, Liu LL, Sun SX, Li YM, Jia L, Ye SL, Yu YX, Dossa K, Luan YP (2022) Leaf-transcriptome profiles of *phoebe bournei* provide insights into temporal drought stress responses. Front Plant Sci 13:1010314

Lin YX, Jiang HY, Chu ZX, Tang XL, Zhu SW, Cheng BJ (2011) Genome-wide identification, classification and analysis of heat shock transcription factor family in maize. BMC Genomics 12(1):76

Lin Q, Jiang Q, Lin JY, Wang DL, Li SJ, Liu CR, Sun CD, Chen KS (2015) Heat shock transcription factors expression during fruit development and under hot air stress in Ponkan (Citrus reticulata Blanco cv. Ponkan) fruit. Gene 559(2):129–136

Livak KJ, Schmittgen TD (2001) Analysis of relative gene expression data using real-time quantitative PCR and the 2(-Delta Delta C(T)) method. Methods 25(4):402–408

Marchler-Bauer A, Bo Y, Han LY, He JE, Lanczycki CJ, Lu SN, Chitsaz F, Derbyshire MK, Geer RC, Gonzales NR, Gwadz M, Hurwitz DI, Lu F, Marchler GH, Song JS, Thanki N, Wang ZX, Yamashita RA, Zhang DC, Zheng CJ, Geer LY, Bryant SH (2016)

CDD/SPARCLE: functional classification of proteins via subfamily domain architectures. Nucleic Acids Res 45(D1):D200–D203

Mittal D, Chakrabarti S, Sarkar A, Singh A, Grover A (2009) Heat shock factor gene family in rice: genomic organization and transcript expression profiling in response to high temperature, low temperature and oxidative stresses. Plant Physiol Biochem 47(9):785–795

Nishizawa A, Yabuta Y, Yoshida E, Maruta T, Yoshimura K, Shigeoka S (2006) *Arabidopsis* heat shock transcription factor A2 as a key regulator in response to several types of environmental stress. Plant J 48(4):535–547

Nover L, Bharti K, Döring P, Mishra S, Ganguli A, Scharf KD (2001) *Arabidopsis* and the heat stress transcription factor world: how many heat stress transcription factors do we need? Cell Stress Chaperones 6(3):177–189

Penfield S (2008) Temperature perception and signal transduction in plants. New Phytol 179(3):615–628

Polle A, Chen S (2015) On the salty side of life: molecular, physiological and anatomical adaptation and acclimation of trees to extreme habitats. Plant Cell Environ 38:1794–1816

Prieto-Dapena P, Almoguera C, Personat JM, Merchan F, Jordano J (2017) Seed-specific transcription factor HSFA9 links late embryogenesis and early photomorphogenesis. J Exp Bot 68(5):1097–1108

Ratheesh Kumar R, Nagarajan NS, Arunraj SP, Devanjan S, Rajan VBV, Esthaki VK, D'Silva P (2012) HSPIR: a manually annotated heat shock protein information resource. Bioinformatics 28(21):2853–2855

Sakurai H, Enoki Y (2010) Novel aspects of heat shock factors: DNA recognition, chromatin modulation and gene expression. FEBS J 277(20):4140–4149

Scharf KD, Rose S, Zott W, Schöffl F, Nover L, Schöff F (1990) Three tomato genes code for heat stress transcription factors with a region of remarkable homology to the DNA-binding domain of the yeast HSF. EMBO J 9(13):4495–4501

Scharf KD, Berberich T, Ebersberger I, Nover L (2012) The plant heat stress transcription factor (Hsf) family: structure, function and evolution. Biophys Acta Gene Regul Mech 2:104–119

Shaul O (2017) How introns enhance gene expression. Int J Biochem Cell Biol 91:145–155

Sun TP (2011) The molecular mechanism and evolution of the GA-GID1-DELLA signaling module in plants. Curr Biol 21(9):R338–R345

Tan B, Yan L, Li HN, Lian XD, Cheng J, Wang W, Zheng XB, Wang XB, Li JD, Ye X, Zhang LL, Li ZQ, Feng JC (2021) Genome-wide identification of HSF family in peach and functional analysis of *PpHSF5* involvement in root and aerial organ development. PeerJ 9:e10961

von Koskull-Döring P, Scharf K-D, Nover L (2007) The diversity of plant heat stress transcription factors. Trends Plant Sci 12(10):452–457

Wang XM, Shi X, Chen SY, Ma C, Xu SB (2018) Evolutionary origin, gradual accumulation and functional divergence of heat shock factor gene family with plant evolution. Front Plant Sci 9:71

Wang LL, Liu YH, Chai MN, Chen HH, Aslam M, Niu XP, Qin Y, Cai HY (2021) Genome-wide identification, classification, and expression analysis of the *HSF* gene family in pineapple (*Ananas comosus*). PeerJ 9:e11329

Wang LL, Liu YH, Chai GF, Zhang D, Fang YY, Deng K, Aslam M, Niu XP, Zhang WB, Qin Y, Wang XM (2023) Identification of passion fruit HSF gene family and the functional analysis of PeHSF-C1a in response to heat and osmotic stress. Plant Physiol Biochem 200:107800

Waterhouse AM, Procter JB, Martin DMA, Clamp M, Barton GJ (2009) Jalview Version-a multiple sequence alignment editor and analysis workbench. Bioinformatics 25(9):1189–1191

Yang ZJ, Wu XH, Grossnickle SC, Chen LH, Yu XX, El-Kassaby YA, Feng JL (2020) Formula fertilization promotes *Phoebe bournei* robust seedling cultivation. Forests 11(7):781

Yu T, Bai Y, Liu Z, Wang ZY, Yang QH, Wu T, Feng SY, Zhang Y, Shen SQ, Li Q, Gu LQ, Song XM (2022) Large-scale analyses of heat shock transcription factors and database construction based on whole-genome genes in horticultural and representative plants. Hortic Res. https://doi.org/10.1093/hr/uhac035

Yuan T, Liang JX, Dai JH, Zhou XR, Liao WH, Guo ML, Aslam M, Li SB, Cao GQ, Cao SJ (2022) Genome-wide identification of *Eucalyptus* heat shock transcription factor family and their transcriptional analysis under salt and temperature stresses. Int J Mol Sci 23(14):8044

Zhang J, Liu BB, Li JB, Zhang L, Wang Y, Zheng HQ, Lu MZ, Chen J (2015) *Hsf* and *Hsp* gene families in *Populus*: genome-wide identification, organization and correlated expression during development and in stress responses. BMC Genomics 16(1):181

Zhang JH, Zhu YJ, Pan Y, Huang HH, Li CL, Li GZ, Tong ZK (2018) Transcriptomic profiling and identification of candidate genes in two *Phoebe bournei* ecotypes with contrasting cold stress responses. Trees 32(5):1315–1333

Zhang HM, Zhu JH, Gong ZZ, Zhu JK (2022a) Abiotic stress responses in plants. Nat Rev Genet 23(2):104–119

Zhang Q, Geng J, Du YL, Zhao Q, Zhang WJ, Fang QX, Yin ZG, Li JH, Yuan XK, Fan YR, Cheng X, Du JD (2022b) Heat shock transcription factor (Hsf) gene family in common bean (*Phaseolus vulgaris*): genome-wide identification, phylogeny, evolutionary expansion and expression analyses at the sprout stage under abiotic stress. BMC Plant Biol 22(1):33

Zhao K, Dang H, Zhou LD, Hu J, Jin X, Han YZ, Wang SJ (2023) Genome-wide identification and expression analysis of the HSF gene family in *Poplar*. Forests 14(3):510

Zupanska AK, LeFrois C, Ferl RJ, Paul AL (2019) HSFA2 functions in the physiological adaptation of undifferentiated plant cells to spaceflight. Int J Mol Sci 20(2):390

Publisher's Note Springer Nature remains neutral with regard to jurisdictional claims in published maps and institutional affiliations.